A switch in infected erythrocyte deformability at the maturation and blood circulation of Plasmodium falciparum transmission stages.

Marta Tiburcio, Makhtar Niang, Guillaume Deplaine, Sylvie Perrot, Emmanuel Bischoff, Papa Alioune Ndour, Francesco Silvestrini, Ayman Khattab, Genevieve Milon, Peter H. David, et al.

Blood First Edition Paper, prepublished online April 18, 2012; DOI 10.1182/blood-2012-03-414557

A switch in infected erythrocyte deformability at the maturation and blood circulation of *Plasmodium falciparum* transmission stages

Marta Tibúrcio[1†], Makhtar Niang[2†], Guillaume Deplaine[3], Sylvie Perrot[4], Emmanuel Bischoff[5], Papa Alioune Ndour[3], Francesco Silvestrini[1], Ayman Khattab[6], Geneviève Milon[7], Peter H. David[4], Max Hardeman[8], Kenneth D. Vernick[5], Robert W. Sauerwein[9], Peter R. Preiser[2], Odile Mercereau-Puijalon[4], Pierre Buffet[3], Pietro Alano[1*], Catherine Lavazec[4,5**]

[1] Dipartimento di Malattie Infettive, Parassitarie e Immunomediate, Istituto Superiore di Sanità, Rome, Italy.

[2] Nanyang Technological University, School of Biological Sciences, Singapore, Singapore.

[3] INSERM-UPMC, UMR 945, Paris, France.

[4] Département de Parasitologie Mycologie; Unité d'Immunologie Moléculaire des Parasites, CNRS, URA 2581, Institut Pasteur, Paris, France.

[5] Département de Parasitologie Mycologie; Unité de Génétique et Génomique des Insectes Vecteurs, CNRS, URA 3012, Institut Pasteur, Paris, France.

[6] Department of Bacteriology and Immunology, Haartman Institute, University of Helsinki, Helsinki, Finland.

[7] Département de Parasitologie Mycologie; Immunophysiologie et Parasitisme, Institut Pasteur, Paris, France.

[8] Department of Translational Physiology, Academic Medical Center, Amsterdam, The Netherlands.

[9] Department of Medical Microbiology, Radboud University Nijmegen Medical Centre, Nijmegen, The Netherlands.

[†] These authors contributed equally to this manuscript

Corresponding authors:

* Pietro Alano : alano@iss.it, Tel. (+39) 064990 2868; Fax (+39) 064990 2226

** Catherine Lavazec : clavazec@pasteur.fr; Tel: (+33) 144389435; Fax: (+33) 140613471

Running title: Switch in deformability in *Plasmodium* gametocytes

Abstract

Achievement of malaria elimination requires development of novel strategies interfering with parasite transmission, including targeting the parasite sexual stages (gametocytes). The formation of *Plasmodium falciparum* gametocytes in the human host takes several days during which immature Gametocyte-Infected Erythrocytes (GIE) sequester in host tissues. Only mature stage GIEs circulate in the peripheral blood, available to uptake by the *Anopheles* vector. Mechanisms underlying GIE sequestration and release in circulation are virtually unknown. We show here that mature GIE are more deformable than immature stages using ektacytometry and microsphiltration methods, and that a switch in cellular deformability in the transition from immature to mature gametocytes is accompanied by the de-association of parasite-derived STEVOR proteins from the infected erythrocyte membrane. We hypothesize that mechanical retention contributes to sequestration of immature GIE and that regained deformability of mature gametocytes is associated with their release in the bloodstream and ability to circulate. These processes are proposed to play a key role in *P. falciparum* gametocyte development in the host and to represent novel and unconventional targets for interfering with parasite transmission.

Introduction

An essential step in the achievement of malaria elimination is to block the transmission of sexual stages parasites, the gametocytes, to the mosquito vector. In the case of *Plasmodium falciparum*, causing the most lethal form of malaria, gametocyte maturation requires the exceptionally long time of 8-10 days, compared to the 48h asexual cycle, and is conventionally divided in five different morphological stages (I-V).[1] Only the mature stage V circulate in the peripheral blood, whilst immature Gametocyte-Infected Erythrocytes (GIE) from stage II to IV have been reported to sequester in internal organs such as the bone marrow and the spleen.[2,3] Although profound morphological changes, accompanied by expression of 2-300 sexual stage specific transcripts and proteins, have been described in gametocytogenesis,[4-6] the mechanisms of GIE sequestration, and the relative contribution of cytoadherence and changes in GIE deformability in this process are virtually unknown.

Proposed mechanisms of *P. falciparum* sequestration mainly derive from studies on the pathogenic asexual stages. These circulate in the bloodstream as "ring" stages in the first 24h post-erythrocyte invasion, and then sequester in various organs to complete maturation to schizont stages, which burst to produce the next generation of free circulating ring forms. Asexual parasite sequestration is mediated by parasite induced modifications of the erythrocyte surface called knobs, enabling the interaction of *P. falciparum* erythrocyte membrane protein 1 (PfEMP1) with host ligands on microvasculature endothelial cells. Absence of knobs in gametocytes from stage II to V[5] and their failure to adhere to endothelial cell lines[7] as well as failure to detect PfEMP1 on the surface of erythrocytes infected by stage III and IV gametocytes[8-11] suggest however that maintenance of sequestration of immature GIE is mediated by different mechanisms. Other families of genes involved in host cell modification such as RIFINs and STEVORs are expressed during gametocytogenesis,[12,13] but a functional role for such proteins in sexual differentiation has

not yet been demonstrated. STEVOR proteins, produced by transcripts expressed early in gametocytogenesis, are trafficked to the infected erythrocyte membrane during gametocyte maturation.[12] STEVORs have been recently shown to strongly impact deformability of erythrocytes hosting asexual *P. falciparum* parasites.[14]

In this work we analyzed the rheological properties of GIE at various stages of development, complementing such observations with a molecular and cellular analysis of STEVOR expression and localization during gametocytogenesis. Ektacytometry and microsphiltration methods were combined here for the first time to measure GIE deformability and filterability, respectively, of *P. falciparum* gametocytes. Such technically diverse approaches indicated that immature GIE are poorly deformable and revealed that mature stage V GIEs are significantly more deformable than immature GIE. Moreover, we show that STEVOR proteins contribute to the overall stiffness of immature GIE, and that the observed switch in cellular deformability is linked to the de-association of STEVORs from the erythrocyte membrane in mature gametocytes.

Materials and Methods

Gametocyte culture and stage specific purification

The *P. falciparum* clonal lines 3D7, B10, H4 and A12 as well as the transgenic lines SFM (Stevor-Flag-c-Myc), 2TMFM (Pfmc-2TM-FLAG-myc) and 3D7GFP have been described elsewhere.[4,15,16] All derive from the NF54 line. Parasites were cultivated *in vitro* under standard conditions using RPMI 1640 medium supplemented with 10% heat-inactivated human serum and human erythrocytes at a 5% haematocrit.[17] Synchronous production of gametocytes stages was achieved as described.[18] For the isolation of gametocytes, culture medium was supplemented with 50mM *N*-acetylglucosamine (GlcNAc) from day 0 onwards and medium replacement was continued for 2 to 5 days to eliminate the asexual stages. Gametocytes were enriched by Percoll gradient or by magnetic isolation using a MACS depletion column (Miltenyi Biotec) in conjunction with a magnetic separator.

Immature GIE from patient blood

A 42 year-old patient was treated with quinine for severe malaria attack with impaired consciousness, renal failure and 4% initial parasitaemia comprising a large proportion of mature trophozoites and schizonts and a smaller proportion of immature gametocytes. Howell-Jolly bodies, a marker of hyposplenism, were evident in 0.3% of red blood cells thereby explaining the very unusual aspect of the thin smear. Immunochromatography and PCR confirmed that the patient was infected exclusively with *P. falciparum.* At day 3 and day 4 of quinine therapy, blood was collected to assess parasite clearance and sent the same day to the National Reference Center for Malaria. Thin smears showed complete clearance of asexual stages and the persistence of immature GIE (stages II-IV). Blood samples were washed 3 times with RPMI medium to remove leucocytes and immediately submitted to microsphiltration as described. GIE were staged and enumerated on 200 high-power (x1000) fields and the retention rate calculated as described. Patient consent was obtained by the

attending physician before blood collection as per National Reference Center standard operating procedure.

Ektacytometry measurement of GIE population elongation index

Deformability measurements of GIE populations were carried out using ektacytometry analysis via Laser-assisted optical rotational cell analyzer (LORCA).[19] The extent of erythrocyte deformability, or elongation index (EI), was defined as the ratio between the difference of the 2 axes of the ellipsoid diffraction pattern and the sum of these 2 axes. Populations of GIE stage II/III and stage V, at 40% parasitaemia and 40% hematocrit in a final volume of 25 µL were diluted in isotonic solutions of polyvinylpyrrolidone (PVP) and were exposed to increasing shear stresses from 0 to 30 Pa, at 37ºC, as described.[19] Gametocytes were enriched by multilayer percoll gradient from synchronized cultures. At least two independent experiments were performed for each GIE stage. Each independent experiment included a Percoll treated population of uninfected erythrocytes, from the same batch, and kept in culture for the same time of the GIE, at 40% hematocrit in a final volume of 25 µL. Direct microscopic observation of GIE diluted in PVP was performed before and after LORCA measurements and excluded that cell aggregation was occurring in the experiments.

Microsphiltration

Calibrated metal microspheres (96.50% tin, 3.00% silver, and 0.50% copper; Industrie des Poudres Sphériques, Annemasse, France) with 2 different size distributions (5- to 15-µm-diameter and 15- to 25-µm-diameter) comprised a matrix used to assay infected erythrocyte deformability under flow, as recently described.[20,21] Suspensions of synchronized cultures containing 2-5 % GIE were perfused through the microsphere matrix at a flow rate of 60 mL/h using an electric pump (Syramed µsp6000, Arcomed' Ag), followed by a wash with 6 mL complete medium. The upstream and downstream samples were collected and smeared

onto glass slides for staining with Giemsa reagent and parasitaemia was assayed to determine parasite retention versus flow through. To visualize GIE shape during their flowing through the matrix, 1 mL of PBS/4% paraformaldehyde was added after perfusion of the GIE-containing culture on the microsphere matrix. After 5 min incubation, fixed GIE were separated from the microspheres by a 3-step decantation procedure, and GIE morphology was observed on a glass slide by light microscopy using a Leica DM 5000 B at 100X magnification.

Scanning Electron microscopy

Before gametocytogenesis induction, the *P. falciparum* B10 clone was selected by gel floatation during several cycles to select for knob-producing parasites. Gametocytes were purified by magnetic isolation and the cell pellets resuspended in 2.5% gluteraldehyde (EM grade) in sodium cacodylate 0.1M, pH 7.2, for 1 h at 4°C. Cells were washed 3 times in sodium cacodylate, transferred to polylysine-coated coverslips and incubated 1 h in 1% osmium tetroxide. After 3 washes in H_2O, samples were dehydrated (25%, 50%, 75%, 95%, 2×100%, 5 minutes each), incubated for 10 min. in acetone, subjected to critical point drying, and coated with platinum in a gun ionic evaporator. Samples were examined and photographed with a JEOL 6700 F electron microscope operating at 2kV.

Immunostaining of fixed and live GIE

Parasites were washed in PBS, air-dried on glass blood smears and methanol- or acetone-fixed for 5-15 min. After 1h pre-incubation in 1% BSA, parasites were incubated with one of the following antisera: anti-STEVOR mouse antiserum (mouse anti-S2) diluted 1:400, [22] a pool of mouse antisera against four STEVOR proteins (anti-PFA0750w, -PFL2610w, -MAL13P1.7 or -PFC0025c) diluted 1:500 ,[23] an anti-Pfg27 rabbit antiserum diluted 1:100, [24] or an anti-c-myc rat monoclonal antibody diluted 1:500 (SantaCruz BiotechnoloGIE). After washes in 1X PBS, slides were incubated with Alexa Fluor conjugated secondary antibody

against either rat, rabbit or mouse IgGs (Molecular Probes) containing DAPI (2µg/mL). Samples were observed at 100X magnification using a Leica DM 5000 B or an Olympus fluorescent microscope. Immunostaining of live GIE was performed on MACS purified GIE washed in RPMI, re-suspended in binding buffer (RPMI/10% FBS) and diluted to 5% parasitemia with uninfected erythrocytes. 50µL of cell suspension were incubated for 1h at 4°C in a rotating wheel with rabbit anti-STEVOR (rabbit anti-S2)[25] and mouse monoclonal anti-Glycophorin C (GPC, vCell Science, Singapore) diluted 1:400 and 1:500 respectively. For detection of Pfg27 and/or STEVOR internal proteins, infected erythrocytes were permeabilized by addition of 3-4 heamolytic units of Streptolysin O (SLO, Sigma Chemical Co, U.S.A.) as described.[26] After 3 washes in RPMI, parasites were incubated 1h with Alexa Fluor conjugated secondary antibody against either rabbit or mouse IgGs (Molecular Probes) containing DAPI (2µg/mL). Samples were mounted in vectashield onto a glass slide and visualized with Olympus fluorescence microscope at 100X magnification.

Immunoblotting analysis

GIE were purified by magnetic isolation and denatured in protein loading buffer 5 min at 100°C. Samples (5.10^6 parasites/lane) were separated by 4-12% SDS-PAGE, transferred to PVDF membrane and blocked for 1 h in 5% nonfat dry milk. Immunoblots were probed with a pool of mouse antiserum against STEVOR proteins (anti-PFA0750w, -PFL2610w, -MAL13P1.7 or -PFC0025c) at 1:3000,[23] a mouse mAb anti-HSP70 antibody at 1/5000, followed by 1 hour with horseradish peroxidase-conjugated anti-mouse IgG secondary antibodies (Promega) at 1:25 000. Detection step was performed using the Pierce chemoluminescence system (Pierce) following the manufacturer's instructions.

Statistical analysis

Statistical significance for differences in elongation indexes and retention rates were established using Wilcoxon Mann-Whitney rank sum test. Statistical significance for

differences in proportion of GIE showing different shape was established using a Chi-square test.

Results

Mature GIE are more deformable than immature GIE

Scanning electron microscopy of the conventionally described stages of gametocyte maturation[1,5] showed the evolution from a convex half moon-like shape in stage II to an elongated shape in stage III, followed by a crescent shape with protruding extremities in stage IV, finally leading to an elongated and curved shape with smooth ends in the mature stage V (Figure 1A). Interestingly, the process is accompanied by an increasing transparency of the residual portion of erythrocyte cytoplasm (Laveran's bib), consistent with the reported decrease in hemoglobin concentration in developing gametocytes.[27] To investigate whether these morphological changes are associated with changes in mechanical properties of infected cells, we used ektacytometry via Laser-assisted optical rotational cell analyzer (LORCA). In these experiments, the elongation index (EI) is measured in response to increasing shear stress (SS) from 0 to 30 Pa, with higher EI corresponding to increased GIE deformability. Cell samples containing 40% infected erythrocytes with either immature (II/III) or mature (V) 3D7 gametocyte stages were compared (Figure 1B). Result of these experiments was that mature GIE populations consistently showed higher EI values over all SS compared to the immature GIE samples in independent biological replicates (Figure 1C). In order to eliminate interference of factors such as blood source or culture time, the average ratio for EI of infected vs uninfected erythrocytes was calculated for each SS. In the SS range from 3 to 9,49 Pascal, more sensitive to detect differences in deformability between erythrocyte populations compared to higher SS,[28] ratio was significantly lower (P =.0004) for stage II/III GIE compared to the mature stage V GIE (Figure 1D). Significantly different ratios persisted at higher SS (Supplemental Figure S1), although both cell types tended to reach closer EI values at maximum SS of 30 Pascal, a phenomenon previously observed in studies on blood diseases where erythrocytes present decreased deformability.[28] In

summary, these results clearly indicate that mature GIE are significantly more deformable than erythrocytes containing the immature II/III sexual stages.

A switch in deformability and filterability of GIE occurs at the transition between immature and mature gametocytes

In order to evaluate GIE mechanical properties in an independent and technically diverse approach, the filterability of GIE using the microsphiltration method was analysed. This technique measures deformability of parasitized erythrocyte flowing through a defined matrix of microspheres that contains narrow and short apertures, and was validated against *ex vivo* perfused human spleen.[20,21] As this method mimics the physical constrains experienced by infected erythrocytes in the splenic microcirculation, it was used to investigate whether changes in GIE deformability during gametocytogenesis correlated with the ability of different gametocyte stages to circulate in peripheral blood. In this system, increased retention rates and impaired filterability correspond to decreased erythrocyte deformability.[29] Retention rates were monitored for synchronous cultures of stage II, III, IV, and V gametocytes from three different parasite clones (Figure 2A). In all parasite lines, immature GIE (stages II to IV) displayed high retention rates ranging from 72% to 96%. Experiments with immature GIE (stages II to IV) from the blood of a hyposplenic patient confirmed this high retention rate (75% to 100% retention), indicating that this property is not due to an *in vitro* artefact linked to gametocyte cultivation. In marked contrast, mature stages were substantially more deformable since less than 23% of stage V GIE were retained on the microspheres ($P < .00001$). Analysis of Giemsa stained smears of mature gametocytes upstream and downstream the microsphere matrix showed a similar male:female ratio for the two samples. To visualize the shape of GIE as they flow through the matrix we added a paraformaldehyde-fixation step in the microsphiltration experiment. This showed that 82% of observed immature stages maintained their convex shape, whereas

75% of mature gametocytes displayed a twisted, elongated dumbbell-like shape likely reflecting their ability to squeeze and slide between microspheres (Figures 2B and 2C). These results clearly confirm the observations obtained by ektacytometry that mature GIE are significantly more deformable than immature GIE. Importantly, microsphiltration experiments in addition reveal that a major switch in GIE deformability occurs at the transition between stage IV and stage V, which coincides with the release from the sequestration sites and the restored ability to circulate of the mature stages.

The switch in deformability correlates with a modified STEVOR localization in the erythrocyte

To investigate whether GIE deformability modifications are mediated by changes in expression or location of specific parasite proteins, we focused on parasite gene products known to be expressed during gametocytogenesis and associated with the erythrocyte membrane. Amongst them the members of the STEVOR multigenic family fulfilled these criteria[12,13,15,25] and, importantly, STEVORs were recently shown in asexual stages to impact deformability of the infected erythrocytes.[14] Expression and cellular localisation of STEVORs during gametocyte development was investigated by western-blot and by immunofluorescence using different sets of antibodies. Western-blot analysis using mouse polyclonal sera against a semi-conserved region of STEVOR proteins[25] showed that STEVOR abundance was stable from stage II to V GIE (Supplemental Figure S2). Immunofluorescence analysis of acetone-fixed GIE using the same antibodies confirmed the presence of STEVOR from stage II to V GIE (Figure 3A). STEVOR-specific fluorescence was progressively exported to the erythrocyte cytoplasm of stage III and stage IV GIE, in which a dotted pattern co-localizing with the erythrocyte membrane was clearly visible. In stage V gametocytes the STEVOR signal was mainly associated to the gametocyte cytoplasm, co-localizing with the signal from the gametocyte internal protein Pfg27 (Figure

3A).[30] Such a differential distribution of STEVORs in immature and mature GIE was confirmed on methanol-fixed GIE using a pool of mouse antisera against four STEVOR proteins (Figure 3 C and 5A).[23] To gain further insights in STEVOR localisation, immunostaining of live GIE showed that STEVORs could be detected on the surface of stages III and IV but not of stage V GIE (Figure 3B). This observation was confirmed as anti-STEVOR antibodies gave a double positive signal with anti-Glycophorin C antibodies only on the surface of immature GIE and not on that of stage V GIE (Supplemental Figure S3). Furthermore, stage V gametocytes positively reacted with anti-STEVOR antibodies only after Streptolysin O permeabilization, confirming that the residual STEVOR-specific signal on mature GIE was due to internally located STEVOR proteins (Supplemental Figure S2). In summary, our data show that the switch in cellular deformability at the transition between immature and mature GIE coincides with a moment in which STEVORs are no longer detectable in association with the erythrocyte membrane. This result suggests that STEVORs mediate a decreased erythrocyte membrane viscoelasticity and contribute to infected cell stiffness in immature GIE, similarly to what observed for erythrocytes infected with asexual stages.[14]

STEVOR expression and localization contributes to GIE deformability

To test this hypothesis, stage-specific GIE deformability was analysed in gametocytes defective in the expression or, on the contrary, overproducing STEVOR proteins. In the first set of experiments the NF54 derived clone A12, in which mRNA production of all *stevor* genes is downregulated during asexual development[16] was used to produce gametocytes. Immunobloting and immunostaining with anti-STEVOR polyclonal sera on methanol-fixed GIE from clone A12 indicated that STEVOR expression was significantly decreased in A12 gametocytes compared to those produced by the sibling B10 and H4 clones (Figure 4A and 4B, supplemental Figure S4). Microsphiltration experiments on immature GIE from these

clones showed similar retention rates in stages II but revealed a significant decrease in retention rates in A12 compared to B10 and H4 in stage III (68.2% vs 96% and 93.8%, *P* =.0051 and.0025) and stage IV GIE (65.8% vs 85.3% and 89%, *P* = .0086 and .0041). Mature GIE showed as expected similar low retention rates in all clones (Figure 4C). In the second set of experiments, STEVOR overproduction in gametocytes was achieved in the transgenic parasite line STEVOR-Flag-c-myc (SFM), which overexpresses a c-myc-tagged copy of the PFF1550w *stevor* gene driven by the *hrp3* promoter.[15] Immunoblotting showed that STEVORs were more abundant in SFM than in wild-type gametocytes (Figure 5B). Importantly, immunostaining with anti-STEVOR polyclonal sera and an anti-c-myc mAb on methanol-fixed GIE in the SFM line revealed that the overexpressed STEVOR protein was partly localised at the infected erythrocyte membrane also in stage V GIE (Figure 5A). Microsphiltration analysis of synchronous wild-type and SFM gametocytes showed that retention rates were similar at the stages II and III, and slightly higher in SFM parasites at stage IV (*P* = .03). However, the retention rate of stage V GIE was substantially higher in SFM than in wild-type parasites (78% vs 23%, *P* = .00001), suggesting that STEVOR overexpression and its persistence at the erythrocyte membrane in stage V GIE significantly impaired the increase in deformability associated with wild-type GIE maturation (Figure 5C). In order to exclude that retention of SFM stage V was due to delayed sexual maturation, stage V gametocytes were tested for their exflagellation efficiency. Result was that SFM stage V exflagellated with the same kinetics and efficiency as wild-type gametocytes (not shown). To control for possible artifactual increase in the rigidity of SFM stage V GIE resulting from transgene overexpression, gametocytes overproducing a c-myc-tagged member of the *Pf*mc-2TM family, obtained from the transgenic line 2TMFM, were analysed. Retention rates for 2TMFM GIE were similar to those of the wild-type line at all

stages, indicating that the increased retention rates of mature SFM GIE were specifically linked to STEVOR overexpression (Figure 5C).

Discussion

We investigated changes in deformability and filterability of erythrocytes infected with immature and mature gametocytes of *P. falciparum*. Our results establish that immature GIE are poorly deformable, and that a switch in deformability occurs at the transition from immature to mature GIE. In human infections this developmental step coincides with the appearance of mature gametocyte in circulation after release from their yet unknown sequestration sites in the body, and with their restored ability to circulate in blood and to cross narrow capillaries and splenic slits. Microsphiltration results reported here establish that erythrocytes infected by immature gametocytes exhibit high retention rates comparable to those of mature asexual stages. In contrast, mature GIE displayed deformability properties similar to those of erythrocytes infected with the freely circulating ring stage parasites.[14] The independent technical approach of ektacytometry in our work and in a recent report[31] also showed that mature GIE are significantly more deformable than immature GIE, confirming the microsphiltration experiments. These results are altogether consistent with the need for mature gametocytes to cross the splenic slits in order to circulate, a prerequisite to be ingested by *Anopheles* and ensure transmission. We show here that the STEVOR family plays a role in this process, as immature gametocytes underexpressing such proteins display an increased deformability compared to wild type immature stages, and gametocytes overexpressing STEVORs remain poorly deformable also at the mature stage.

The integration in the present work of observations on whole GIE mechanical properties, gametocyte morphology, and dynamic association of parasite molecules with the erythrocyte membrane provides the first clues on the mechanisms governing the developmental changes

in GIE deformability. Changes in mechanical properties of *P. falciparum* infected erythrocytes result from the combination of presence of the intracellular parasite and parasite-induced modifications of its erythrocyte host. Erythrocyte deformability is determined by three factors: the surface area and volume of the cell, the cytoplasmic viscosity and the membrane viscoelasticity.[32] The altered morphology of GIE fixed inside the microsphere matrix shows that mature gametocytes themselves are, unlike the immature stages, highly stretched within the erythrocyte, suggesting an increase in intrinsic parasite deformability during sexual maturation. A process likely to be responsible for such a modification is the disassembly of the microtubular subpellicular network subtending the trilaminar membrane structure in the transition from stage IV to stage V gametocytes. [5] Recent cryo X-ray tomography analysis revealed that the surface area and the volume of GIE remain roughly constant during gametocyte development,[27] suggesting limited impact of these factors on the observed switch in deformability at the transition from stage IV to stage V. The same study also showed that about 70% of the erythrocyte hemoglobin is digested during gametocytogenesis. As this decrease is progressive throughout sexual development, it is unlikely that changes in GIE cytoplasmic viscosity entirely account for the abrupt switch in deformability at the transition between stage IV and V GIE. It is therefore plausible that decreased membrane viscoelasticity contributes to stiffness of immature GIE, which, based on observations with asexual stages,[33] is likely a consequence of mediated by parasite-encoded proteins associating with the erythrocyte membrane skeleton.

The findings that STEVORs associate with the erythrocyte membrane in immature GIE and that their disappearance from that site coincides with the increased deformability of mature GIE suggest that these trans-membrane proteins significantly contribute to the decrease in membrane viscoelasticity of immature GIE. The mechanisms underlying STEVOR-

mediated stiffness remain elusive. A possible interaction with erythrocyte cytoskeletal proteins may induce spectrin cross-linking, as proposed for the plasmodial proteins KAHRP and PfEMP3 exported in asexual stages.[34-36] De-association from the erythrocyte membrane in mature stages may result from proteolytic cleavage or conformational changes upon post-translational modifications. Such events are likely responsible for the failure of our antibodies to detect STEVOR association with the erythrocyte membrane in mature GIE, although this was observed using a different set of antibodies raised to small peptides.[12]

Which are the sites of *P. falciparum* gametocyte sequestration in the human body, how immature gametocytes hide in such sites for almost ten days, how do mature stages regain access to blood circulation and which are the mechanisms ensuring their persistence in peripheral circulation for several days are still major unanswered fundamental questions in the biology of malaria parasites. Although a mechanistic hypothesis on gametocyte sequestration is virtually impossible without the identification of the sites of sexual stage sequestration *in vivo*, our results allow us to speculate that immature GIE stiffening and the increase in GIE deformability at gametocyte maturation may be functionally linked with the dynamics of this phenomenon. Once sequestration is established by the round, trophozoite-like stage I gametocytes through yet elusive mechanism(s), we hypothesize that mechanical retention may significantly contribute to maintenance of sequestration throughout the ensuing maturation process of GIE. This is consistent with the fact that PfEMP1 and knob structures are absent from the surface of stage II to V GIE,[5,8] and that immature GIE show only weak, if any, binding interactions with endothelial host cells.[7,8,11] Observations from post mortem and *ex vivo* specimens and from rare clinical cases altogether indicating that bone marrow and spleen are the organs where immature gametocytes are more readily found,[2,3,37] suggest that mechanical retention of immature gametocytes may be favoured in such tissues, characterized by an open and slow blood circulation. A role of adhesins in

gametocyte sequestration cannot however be presently excluded. Recent findings that STEVORs have adhesive properties and are involved in rosetting in asexual stages (Niang et al, unpublished results), and our observation that STEVORs is accessible to antibodies on the GIE surface up to stage IV may suggest a more direct role of such proteins in GIE cytoadhesion, requiring further studies.

Our results suggest that the high deformability specifically characterising stage V GIE may facilitate release from sequestration sites. Importantly, we propose that such a property restores the ability of mature GIE to cross narrow apertures and allows them to escape mechanical retention in the spleen, thus contributing to their sustained circulation in the peripheral blood where they are available to the insect vector for several days. We propose that interventions targeting these processes, thereby reducing the ability of mature GIE to circulate, open novel avenues in the present strategies to reduce parasite transmission.

Acknowledgements

MT and PA acknowledge the financial support from the EU FP7 Marie Curie ITN InterMalTraining, and contract PITN-GA-2008-215281. OMP and PA acknowledge the FP7 NoE EVIMalaR, contract 242095. MN and PRP acknowledge the financial support from the BioMedical Research Council Singapore grant. CL, KV, GM, PB and OMP received financial support from the Région Ile de France, the Fondation Symphasis, the NIH Project "Mechanisms of Erythrocytic Infection and Anemia in Malaria" (Award Number 5P01HL078826-06). We are grateful to François Lacoste (Fondation Ackerman-Fondation de France) for fruitful discussions and financial support.

Conflict-of-interest disclosure

The authors declare no competing financial interests.

Author contributions

MT, MN, GD, SP, PAN, FS, and CL performed experiments, MT, MN, PA and CL analyzed results and made figures; EB performed statistical analysis; AK, GM, MH, KV, RS, OMP, and PB analyzed data and contributed vital new reagents or analytical tools; MT, MK, PP, PD, PA and CL designed the research, MT, PA and CL wrote the paper.

References

1. Hawking F, Wilson ME, Gammage K. Evidence for cyclic development and short-lived maturity in the gametocytes of *Plasmodium falciparum. Trans R Soc Trop Med Hyg.* 1971;65(5):549-559.
2. Bastianelli G, Bignami A. Studi Sulla Infezione Malarica. *Bullettino R Accademia Med* 1893;20:151–220.
3. Smalley ME, Abdalla S, Brown J. The distribution of *Plasmodium falciparum* in the peripheral blood and bone marrow of Gambian children. *Trans R Soc Trop Med Hyg.* 1981;75(1):103-105.
4. Silvestrini F, Lasonder E, Olivieri A, et al. Protein export marks the early phase of gametocytogenesis of the human malaria parasite *Plasmodium falciparum. Mol Cell Proteomics.* 2010;9(7):1437-1448.
5. Sinden RE. Gametocytogenesis of *Plasmodium falciparum in vitro*: an electron microscopic study. *Parasitology.* 1982;84(1):1-11.
6. Young JA, Fivelman QL, Blair PL, et al. The *Plasmodium falciparum* sexual development transcriptome: a microarray analysis using ontology-based pattern identification. *Mol Biochem Parasitol.* 2005;143(1):67-79.
7. Silvestrini F, Tiburcio M, Bertuccini L, Alano P. Differential adhesive properties of sequestered asexual and sexual stages of *Plasmodium falciparum* on human endothelial cells are tissue independent. *PLoS One.* 2012;in press.
8. Day KP, Hayward RE, Smith D, Culvenor JG. CD36-dependent adhesion and knob expression of the transmission stages of *Plasmodium falciparum* is stage specific. *Mol Biochem Parasitol.* 1998;93(2):167-177.
9. Hayward RE, Tiwari B, Piper KP, Baruch DI, Day KP. Virulence and transmission success of the malarial parasite *Plasmodium falciparum. Proc Natl Acad Sci U S A.* 1999;96(8):4563-4568.
10. Rogers NJ, Daramola O, Targett GA, Hall BS. CD36 and intercellular adhesion molecule 1 mediate adhesion of developing *Plasmodium falciparum* gametocytes. *Infect Immun.* 1996;64(4):1480-1483.
11. Rogers NJ, Hall BS, Obiero J, Targett GA, Sutherland CJ. A model for sequestration of the transmission stages of *Plasmodium falciparum*: adhesion of gametocyte-infected erythrocytes to human bone marrow cells. *Infect Immun.* 2000;68(6):3455-3462.
12. McRobert L, Preiser P, Sharp S, et al. Distinct trafficking and localization of STEVOR proteins in three stages of the *Plasmodium falciparum* life cycle. *Infect Immun.* 2004;72(11):6597-6602.
13. Petter M, Bonow I, Klinkert MQ. Diverse expression patterns of subgroups of the *rif* multigene family during *Plasmodium falciparum* gametocytogenesis. *PLoS One.* 2008;3(11):e3779.
14. Sanyal S, Egee S, Bouyer G, et al. *Plasmodium falciparum* STEVOR proteins impact erythrocyte mechanical properties. *Blood*. 2012;119(2):e1-8.
15. Lavazec C, Sanyal S, Templeton TJ. Hypervariability within the *Rifin, Stevor* and *Pfmc-2TM* superfamilies in *Plasmodium falciparum*. *Nucleic Acids Res.* 2006;34(22):6696-6707.
16. Lavazec C, Sanyal S, Templeton TJ. Expression switching in the *stevor* and *Pfmc-2TM* superfamilies in *Plasmodium falciparum. Mol Microbiol.* 2007;64(6):1621-1634.
17. Trager W, Jensen JB. Human malaria parasites in continuous culture. *Science.* 1976;193(4254):673-675.
18. Fivelman QL, McRobert L, Sharp S, et al. Improved synchronous production of *Plasmodium falciparum* gametocytes *in vitro*. *Mol Biochem Parasitol.* 2007;154(1):119-123.

19. Hardeman MR, Goedhart PT, Dobbe JG, Lettinga KP. Laser-assisted Optical Rotational Cell Analyser (L.O.R.C.A): I. A new instrument for measurement of various structural hemorheological parameters. *Clinical Hemorheology*. 1994;14(4):605-618.
20. Deplaine G, Safeukui I, Jeddi F, et al. The sensing of poorly deformable red blood cells by the human spleen can be mimicked *in vitro*. *Blood*. 2011;117(8):e88-95.
21. Lavazec C, Deplaine G, Safeukui I, et al. eds. Microsphiltration: a microsphere matrix to explore erythrocyte deformability. In: Press H ed. *Malaria Methods and Protocols*; in press.
22. Blythe JE, Yam XY, Kuss C, et al. *Plasmodium falciparum* STEVOR proteins are highly expressed in patient isolates and located in the surface membranes of infected red blood cells and the apical tips of merozoites. *Infect Immun*. 2008;76(7):3329-3336.
23. Schreiber N, Khattab A, Petter M, et al. Expression of *Plasmodium falciparum* 3D7 STEVOR proteins for evaluation of antibody responses following malaria infections in naive infants. *Parasitology*. 2008;135(2):155-167.
24. Olivieri A, Camarda G, Bertuccini L, et al. The *Plasmodium falciparum* protein Pfg27 is dispensable for gametocyte and gamete production, but contributes to cell integrity during gametocytogenesis. *Mol Microbiol.* 2009;73(2):180-193.
25. Niang M, Yan Yam X, Preiser PR. The *Plasmodium falciparum* STEVOR multigene family mediates antigenic variation of the infected erythrocyte. *PLoS Pathog*. 2009;5(2):e1000307.
26. Ansorge I, Benting J, Bhakdi S, Lingelbach K. Protein sorting in *Plasmodium falciparum*-infected red blood cells permeabilized with the pore-forming protein streptolysin O. *Biochem J*. 1996;315 (Pt 1):307-314.
27. Hanssen E, Knoechel C, Dearnley M, et al. Soft X-ray microscopy analysis of cell volume and hemoglobin content in erythrocytes infected with asexual and sexual stages of *Plasmodium falciparum. J Struct Biol.* 2012;177(2):224-32.
28. Hardeman MR, Ince C. Clinical potential of *in vitro* measured red cell deformability, a myth? *Clin Hemorheol Microcirc*. 1999;21:277-284.
29. Baskurt OK, Boynard M, Cokelet GC, et al. New guidelines for hemorheological laboratory techniques. *Clin Hemorheol Microcirc*. 2009;42(2):75-97.
30. Camarda G, Bertuccini L, Singh SK, et al. Regulated oligomerisation and molecular interactions of the early gametocyte protein Pfg27 in *Plasmodium falciparum* sexual differentiation. *Int J Parasitol*. 2010;40(6):663-673.
31. Dearnley MK, Yeoman JA, Hanssen E, et al. Origin, composition, organization and function of the inner membrane complex of *Plasmodium falciparum* gametocytes. *J Cell Sci*. 2012.
32. Mohandas N, Gallagher PG. Red cell membrane: past, present, and future. *Blood*. 2008;112(10):3939-3948.
33. Maier AG, Cooke BM, Cowman AF, Tilley L. Malaria parasite proteins that remodel the host erythrocyte. *Nat Rev Microbiol*. 2009;7(5):341-354.
34. Glenister FK, Coppel RL, Cowman AF, Mohandas N, Cooke BM. Contribution of parasite proteins to altered mechanical properties of malaria-infected red blood cells. *Blood*. 2002;99(3):1060-1063.
35. Pei X, An X, Guo X, Tarnawski M, Coppel R, Mohandas N. Structural and functional studies of interaction between *Plasmodium falciparum* knob-associated histidine-rich protein (KAHRP) and erythrocyte spectrin. *J Biol Chem*. 2005;280(35):31166-31171.
36. Pei X, Guo X, Coppel R, Mohandas N, An X. *Plasmodium falciparum* erythrocyte membrane protein 3 (PfEMP3) destabilizes erythrocyte membrane skeleton. *J Biol Chem*. 2007;282(37):26754-26758.

37. Bachmann A, Esser C, Petter M, et al. Absence of erythrocyte sequestration and lack of multicopy gene family expression in *Plasmodium falciparum* from a splenectomized malaria patient. *PLoS One.* 2009;4(10):e7459.

Figures Legends

Figure 1. Scanning electron microscopy and ektacytometry analysis of immature and mature *P. falciparum* GIE.

A: Scanning electron microscopy images of *P. falciparum* GIE (B10 clone) from stage II to V of maturation. The bars represent 1µm. B: Giemsa staining images of stage II/III (upper panel) and stage V (lower panel) GIE samples used in ektacytometry analysis. C: Response to increasing shear stress of erythrocytes infected by *P. falciparum* stage II/III (red line) and V (blue line) gametocytes (40% parasitaemia) and of uninfected erythrocytes (green line). The error bars indicate standard error. D: Ratios of Elongation Indexes of infected vs uninfected erythrocytes calculated from the 3-9.49 Pascal range of shear stresses in the ektacytometry analysis (C) showing a statistically significant difference between immature and mature GIE (Mann-Whitney rank sum test, $P = .0004$).

Figure 2. Retention in microsphilters of immature and mature GIE

A: Retention in microsphilters of stages II, III, IV and V GIE from different *P. falciparum* clonal lines (B10, H4, 3D7GFP) in culture or directly collected from the blood of a hyposplenic patient treated for a malaria attack (clinic). Immature GIE (stages II-IV) are retained by the microsphilters while mature GIE (stages V) flow through. B: Differential interference contrast images of paraformaldehyde-fixed GIE as they flow through the microsphilters. Immature stages (left panel) keep a convex oval or round shape, unlike uninfected erythrocytes (white star), whereas a majority of mature GIE are twisted and dumbbell-shaped (right panel). C. Graphical representation for the proportion of GIE showing a regular (dark grey) or twisted (light grey) shape in a population of immature (n= 100) and mature (n=36) GIE (Chi-square test, p=1e-9).

Figure 3. Immunofluorescence analysis of STEVOR proteins expression in GIE

A: Analysis of STEVOR proteins expression in fixed II-V-GIE preparations. GIE were acetone-fixed and co-stained with mouse anti-S2 (green) and rabbit anti-Pfg27 (red) followed by anti-mouse Alexa 488- and anti-rabbit Alexa 594-conjugated IgG. Parasite nuclei were stained with DAPI (blue). Bright field (BF) and merge images are shown. The bars represent 2 µm. B: Analysis of live GIE immunostained with rabbit anti-S2 (green) specifically recognizing native STEVOR on the surface of stages III and IV GIE. Bound antibody was detected with anti-rabbit Alexa 488-conjugated IgG. BF, nuclear staining (DAPI, blue) and merge images are shown. C: Immunofluorescence analysis of STEVOR expression in fixed II-V-GIE. GIE were methanol-fixed and stained with a pool of mouse polyclonal antibodies directed against STEVOR proteins followed by anti-mouse Alexa 488-conjugated IgG (green). The bars represent 2 µm.

Figure 4. Decrease in STEVOR expression is associated with an increase in deformability of immature GIE

A: Immunofluorescence analysis of STEVOR expression in stage III and stage IV GIE from the B10, H4 and A12 clones. GIE were stained with a pool of mouse polyclonal antibodies directed against STEVOR proteins followed by anti-mouse Alexa 488-conjugated IgG. Signal intensity was analysed by ImageJ on at least 30 pictures taken under identical exposition conditions for each clone. The bars represent 2 µm. B: Western-blot analysis of STEVOR expression in stage III and stage V GIE from the wild-type and the SFM parasites. Immunoblots were probed with a pool of mouse polyclonal antibodies directed against STEVOR proteins and with a mAb directed against HSP70. C: Retention in microsphilters of stages II, III, IV and V GIE from the B10 (light grey), H4 (dark grey) and A12 (red) clones. Asterisks represent highly significant differences in retention rates ($P < .01$).

Figure 5. Stevor overexpression is associated with a decrease in deformability of mature GIE

A: Immunofluorescence analysis of STEVOR expression in stage III and stage V GIE from the wild-type (WT) and the SFM parasites. GIE were stained with a pool of mouse polyclonal antibodies directed against STEVOR proteins or with anti-c-myc mAb followed by anti-mouse Alexa 488-conjugated IgG. The bars represent 2 µm. B: Western-blot analysis of STEVOR expression in stage III and stage V GIE from the wild-type and the SFM parasites. Immunoblots were probed with a pool of mouse polyclonal antibodies directed against STEVOR proteins and with a mAb directed against HSP70. Vertical lines have been inserted to indicate a repositioned gel lane.

C: Retention in microsphilters of stages II, III, IV and V GIE from different wild-type *P. falciparum* clonal lines (WT representing B10, H4, 3D7GFP clones, in grey), from the SFM parasite line overexpressing a c-myc-tagged copy of the PFF1550w *stevor* gene (green) and the 2TMFM parasite line overexpressing a c-myc-tagged copy of the PFA0680c *Pfmc-2TM* gene (blue). Asterisks represents highly significant differences in retention rates ($P < .01$). NS: Not Significant.

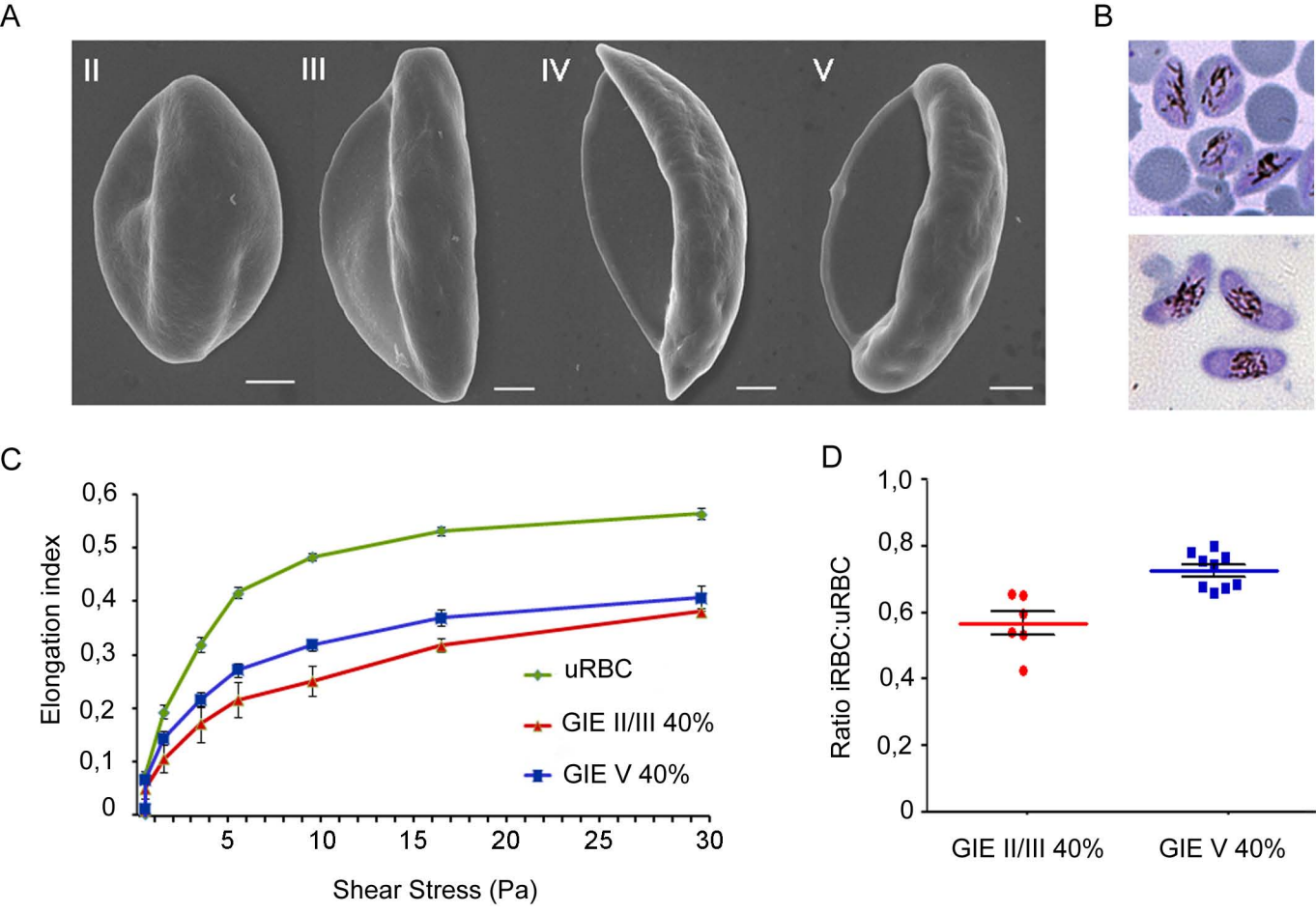
A
II
III
IV
V
B
C
Elongation index
0,6
0,5
0,4
0,3
0,2
0,1
0
5
10
15
20
25
30
Shear Stress (Pa)
uRBC
GIE II/III 40%
GIE V 40%
D
Ratio iRBC:uRBC
1,0
0,8
0,6
0,4
0,2
0
GIE II/III 40%
GIE V 40%

Figure 1

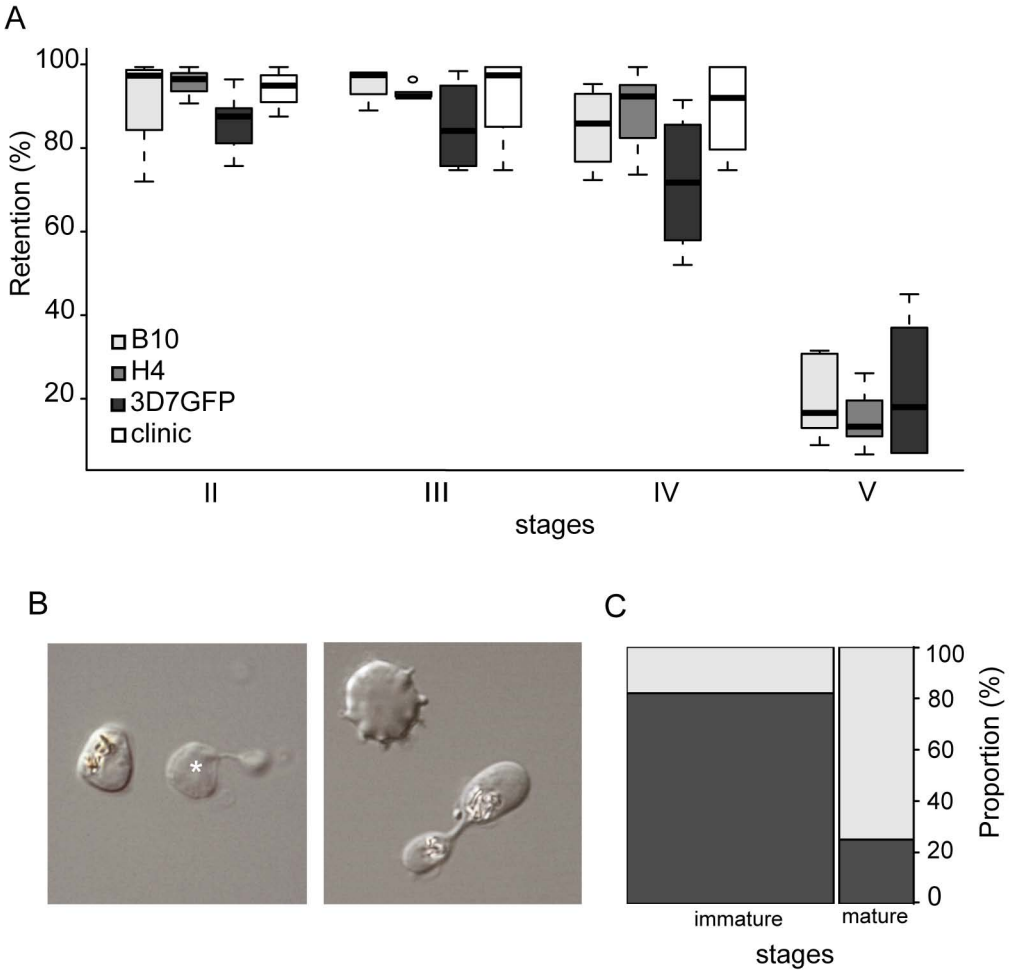
A
100
80
60
40
20
Retention (%)
B10
H4
3D7GFP
clinic
II
III
IV
V
stages
B
C
100
80
60
40
20
0
Proportion (%)
immature
mature
stages

Figure 2

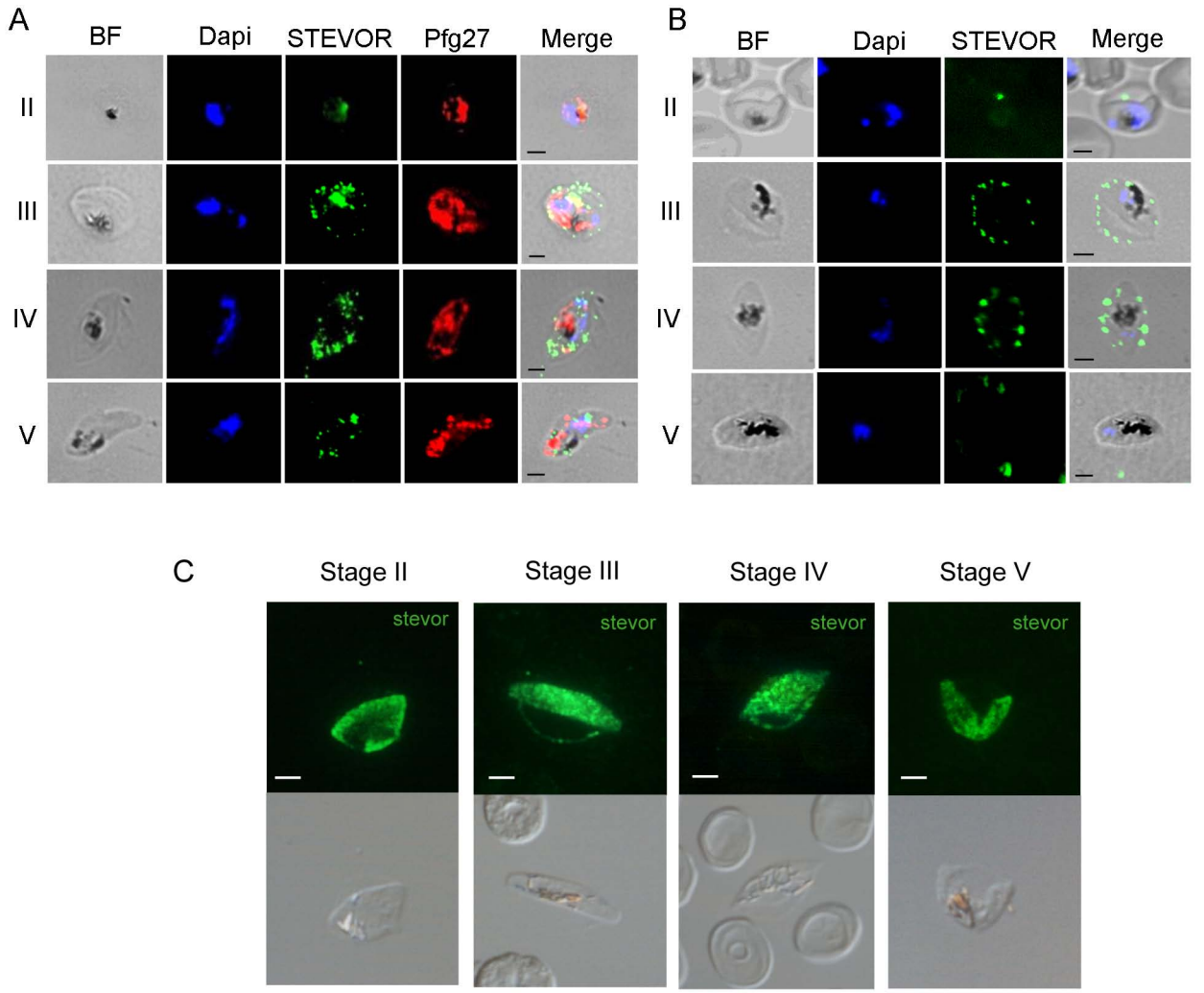
A
BF
Dapi
STEVOR
Pfg27
Merge
II
III
IV
V
B
BF
Dapi
STEVOR
Merge
II
III
IV
V
C
Stage II
Stage III
Stage IV
Stage V
stevor
stevor
stevor
stevor

Figure 3

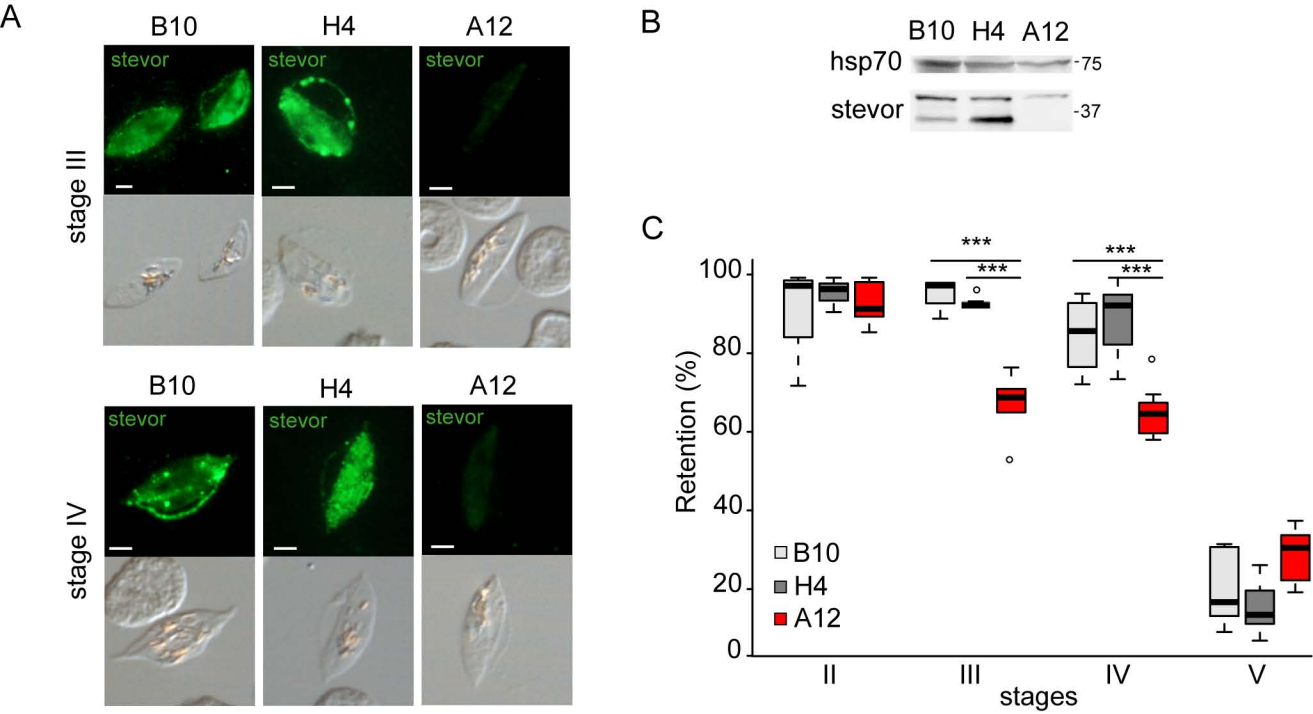
A
B10
H4
A12
stevor
stage III
stage IV
B
B10 H4 A12
hsp70
stevor
-75
-37
C
Retention (%)
100
80
60
40
20
0
***
***
***
***
B10
H4
A12
II
III
IV
V
stages

Figure 4

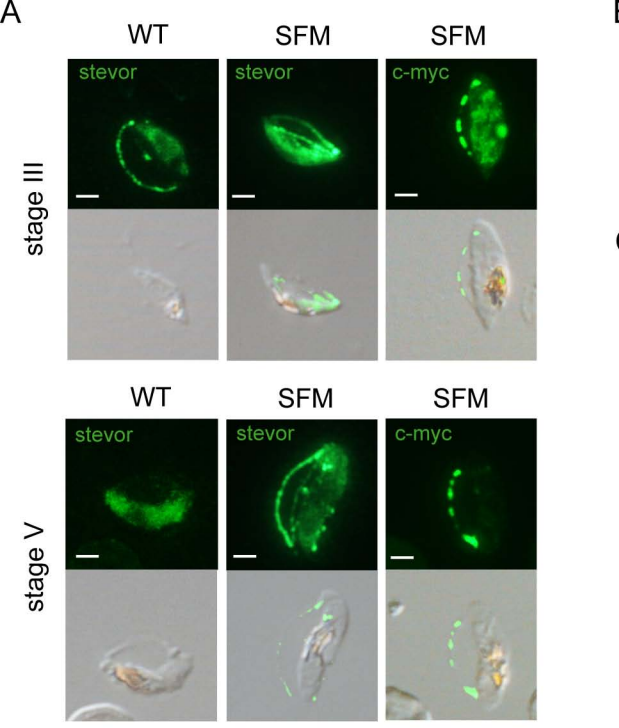
A
WT
SFM
SFM
stevor
stevor
c-myc
stage III
WT
SFM
SFM
stevor
stevor
c-myc
stage V

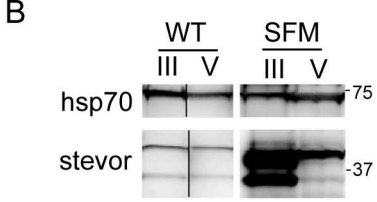
B
WT
SFM
III V
III V
hsp70
stevor
75
37

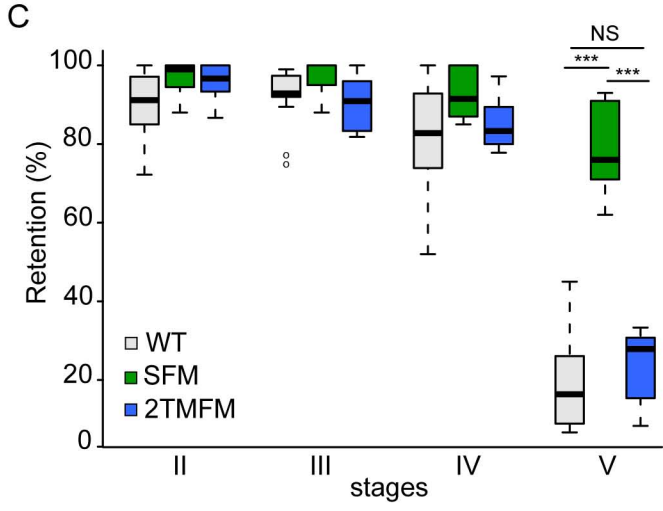
C
NS
***
***
100
80
60
40
20
0
Retention (%)
WT
SFM
2TMFM
II
III
IV
V
stages

Figure 5

Prepublished online April 18, 2012;
doi:10.1182/blood-2012-03-414557

A switch in infected erythrocyte deformability at the maturation and blood circulation of *Plasmodium falciparum* transmission stages

Marta Tibùrcio, Makhtar Niang, Guillaume Deplaine, Sylvie Perrot, Emmanuel Bischoff, Papa Alioune Ndour, Francesco Silvestrini, Ayman Khattab, Geneviève Milon, Peter H. David, Max Hardeman, Kenneth D. Vernick, Robert W. Sauerwein, Peter R. Preiser, Odile Mercereau-Puijalon, Pierre Buffet, Pietro Alano and Catherine Lavazec

Advance online articles have been peer reviewed and accepted for publication but have not yet appeared in the paper journal (edited, typeset versions may be posted when available prior to final publication). Advance online articles are citable and establish publication priority; they are indexed by PubMed from initial publication. Citations to Advance online articles must include digital object identifier (DOIs) and date of initial publication.

Blood (print ISSN 0006-4971, online ISSN 1528-0020), is published weekly by the American Society of Hematology, 2021 L St, NW, Suite 900, Washington DC 20036.